



ELSEVIER

Combustion and Flame 133 (2003) 371–374
Brief communication

Combustion
and Flame

Estimation of the laminar premixed flame temperature and velocity in injection-driven combustion chambers

Anand B. Vyas^a, Joseph Majdalani^{a,*}, Vigor Yang^b

^aMarquette University, Milwaukee, WI 53233, USA

^bPennsylvania State University, University Park, PA 16802, USA

Received 27 March 2002; received in revised form 15 January 2003; accepted 17 January 2003

1. Introduction

Several laminar flame theories have been proposed in the past, the objective of each being the determination of fundamental flame attributes. Classification of these theories has been based on the degree of realism associated with their attendant assumptions, and these are carefully described by Kuo [1] and others [2–4]. Our approach proceeds along the lines of Mallard and Le Châtelier [5], yet differs in some aspects. Whereas Mallard and Le Châtelier divide the flame region into a preheat and a reaction zone, our premixed flame will be treated in a single zone. Furthermore, the chemical reaction rates will be either prescribed or simulated before being introduced into the analytical model as a spatially distributed heat source.

The main objective of this effort is to obtain a closed-form approximation for the steady temperature distribution in a premixed laminar flame inside a planar chamber with porous walls. A premixed flame is often used to simulate solid-propellant burning in core flow studies of injection-driven combustion chambers (see [6] and the companion paper [7]). Our main objective stems from the need to accurately capture the thermal trends reported in the flame zone formed above the surface following propellant pyrolysis. The simplified model to be described will be particularly created to facilitate the merger between the chamber gas dynamics and the heat addition process. The temperature distribution thus approximated

will provide the means to further study the decay or growth mechanisms affecting acoustical and vortical waves near the propellant surface. The current effort is also motivated by the inability of other flame theories to mimic the temperature trends in solid rocket motors (e.g., [8,9]).

A second and equally compelling objective here is to obtain the thermally enhanced velocity v_f directly above the reactive flame zone. In [7], it is shown that $v_{f,r}$ must be used instead of the wall-injection speed v_w in realistic models of the injection-driven combustion field based on nonreactive gas mixtures. A similar but more detailed model was developed by T'ien [10]. However, the temperature distribution obtained by T'ien was found numerically using Runge-Kutta integration. At present, an asymptotic solution will be derived for a model that follows similar lines to those described by T'ien.

In view of the small size of the reactive flame thickness δ_f relative to the radius of an idealized rocket motor chamber [7], curvature effects seem unimportant inside the flame zone. Provided that δ_f remains relatively small, a planar model can arguably provide an adequate approximation of the analogous problem in a chamber with circular cross section. In the interest of simplicity, the planar model will be developed here.

2. Analysis

Using standard descriptors, the differential forms of mass, momentum, and energy conservation can be expressed by

* Corresponding author. Tel.: 414-288-6877; fax: 414-288-7082.

E-mail address: maji@mu.edu (J. Majdalani).

$$\frac{\partial \rho}{\partial t} + \nabla \cdot (\rho \mathbf{u}) = 0 \quad (1)$$

$$\rho \left[\frac{\partial \mathbf{u}}{\partial t} + (\mathbf{u} \cdot \nabla) \mathbf{u} \right] = -\nabla p + \mu \nabla^2 \mathbf{u} \quad (2)$$

$$\rho C_p \left[\frac{\partial T}{\partial t} + (\mathbf{u} \cdot \nabla) T \right] - \left[\frac{\partial p}{\partial t} + (\mathbf{u} \cdot \nabla) p \right] = k \nabla^2 T + \dot{Q} \quad (3)$$

where ρ , p , $\mathbf{u} = (u, v)$, T , and t represent the steady flow density, pressure, velocity, temperature, and time, respectively. While the heat source \dot{Q} is used to represent the net rate of exothermic chemical reactions, the remaining properties represent the specific heat C_p , viscosity μ , and thermal conductivity k .

Equations 1–3 can be simplified based on the assumptions that:

1. The bulk flow is steady.
2. Gradients in temperature normal to the porous walls are much larger than axial gradients ($\partial T/\partial y \gg \partial T/\partial x$). A similar assumption is made for the density gradient. This assumption is consistent with the multidimensional simulation results described in [7].
3. Thermal diffusion is small when compared to thermal convection and heat generation. Such a relative comparison can be accomplished using an order of magnitude analysis. Considering that the thin flame zone becomes even thinner with successive increases in chamber pressure, the diffusion of gas particles crossing the flame zone is virtually insignificant, especially when compared to high speed convection.
4. The velocity inside the flame zone has a negligible axial component because of the no-slip condition at the wall where the parallel x component of \mathbf{u} vanishes. This assumption is justified due to the thin flame zone wherein the axial velocity component can be ignored as the bulk injectants enter perpendicularly to the walls.
5. The bulk velocity outside the flame zone is adequately represented by the isothermal steady flow solution based on the thermally enhanced blowing speed v_f . This steady flow solution has been shown in [7] to provide a sufficiently accurate approximation.
6. As shown by several researchers, the steady pressure gradient is proportional to the square of the injection Mach number. Because the Mach number at the walls is two to three orders of magnitude smaller than unity, the square of the Mach number yields such as

small value that it permits discounting the pressure gradient in the energy equation.

In view of these assumptions, Eqs. 1 and 3 reduce to

$$\frac{\partial(\rho v)}{\partial y} = 0 \text{ or } \rho v = \text{constant} \quad (4)$$

$$\rho v C_p \frac{\partial T}{\partial y} = \dot{Q} \quad (5)$$

The decoupling of the momentum equation can be attributed to the one-dimensionality of the velocity distribution inside the flame zone. Equations 4 and 5 exhibit the following arrangement of boundary conditions:

$$\text{at } y = 0 \quad \rho = \rho_w \quad v = v_w$$

$$T = T_w \text{ (imposed at the porous wall)} \quad (6)$$

$$\text{at } y = \delta_f \quad \rho = \rho_f \quad v = v_f \quad T = T_f \text{ (deduced)} \quad (7)$$

where δ_f is the thickness of the reactive flame zone. Using the same nomenclature as in [7], y denotes the normal coordinate measured from the porous wall.

While conservation of mass dictates that $\rho v = \rho_w v_w$ inside the thin flame zone, conservation of energy cannot be used without providing information regarding the manner in which chemical energy is spatially released over the interval $0 \leq y \leq \delta_f$. The analytical model must be based on the *prescribed form* of heat released by chemical reactions. This form needs to be determined beforehand, either experimentally or by simulation. In [7], for example, the exothermic heat of reaction associated with propane-air combustion is considered. This leads to a typical skewed symmetric function that exhibits a peak value inside the flame zone. Similar heat of reaction curves have been associated with other combusting hydrocarbons [1–4].

The heat release curve determined in [7] can be accurately represented by a Gaussian distribution. Gaussian distributions and error functions have been employed previously to describe both temperature and concentration profiles in several documented studies. Using single reactions and identical species diffusion coefficients, Borghi and Destriau [11] have defined their sum of mass fractions via Shvab-Zeldovich functions that can be represented by Gaussian distributions. Warnatz, Maas, and Dibble [12] have also shown that, for a species transport equation in which convective action is equally matched by diffusion, the solution may be expressed in terms of error functions. For near equi-diffusion flames (NEF) that arise in the vicinity of stagnation points, Buckmaster and Ludford [13] have developed an expression for the temperature profile using error

functions as well. Their solution has been based on the coupled equations representing a balance between species diffusion, thermal diffusion, and convective transport of species and heat. In the current study, the heat source is represented by the Gaussian form

$$\dot{Q}(y) \equiv C_1 + C_2 \exp[-C_3(y - C_4)^2] \quad (8)$$

where the characteristic coefficients $C_i, i = 1, \dots, 4$ can be determined from the heat of formation of diverse species involved in the combustion of a given fuel-oxidizer mixture.

Equation 8 can be substituted into Eq. 5 and integrated. Using Eq. 6 to specify the single temperature boundary condition at the wall, one obtains

$$T(y) = T_w + \frac{2C_1\sqrt{C_3}y + C_2\sqrt{\pi}}{2\sqrt{C_3}\rho v \bar{C}_p} \left\{ \operatorname{erf}(C_4\sqrt{C_3}) + \operatorname{erf}\left[(y - C_4)\sqrt{C_3}\right] \right\} \quad (9)$$

In order to allow for comparisons between Eq. 9 and computations that take into account global chemical kinetics, the numerically generated heat release function obtained in [6,7] is used as an example. Using the method of least-squares, the corresponding coefficients in Eq. 8 are found to be

$$C_1 = 6.34 \times 10^6; C_2 = 1.061 \times 10^9; C_3 = 22.0 \times 10^6; C_4 = 0.00093251 \quad (10)$$

In order to evaluate the temperature distribution, the density and injection velocities at the wall are taken from [6,7] as $\rho_w = 1.02 \text{ kgm}^{-3}$ and $v_w = 0.2 \text{ ms}^{-1}$. The specific heat used in Eq. 9 is approximated by the average specific heat of the reactants. This is due to the flame zone being predominantly occupied by the reactants. The gas products, it has been shown, occupy the majority of the domain outside the flame region. The reactant mixture $C_p(T)$ is determined using the sum of species-specific heats weighed by individual mass fractions. For propane-air reactants, we use

$$C_p(T) = \sum Y_i C_{pi} = Y_{C_3H_8} C_{pC_3H_8} + Y_{O_2} + Y_{N_2} C_{pN_2} \quad (11)$$

where Y_i represents the mass fraction of species i . The average specific heat of the reactants is then calculated from

$$\bar{C}_p = \frac{1}{T_f - T_w} \int_{T_w}^{T_f} C_p dT \quad (12)$$

where, according to [6,7], T_w and T_f are 350 K and 1938 K, respectively.

Having determined the means to approximate the

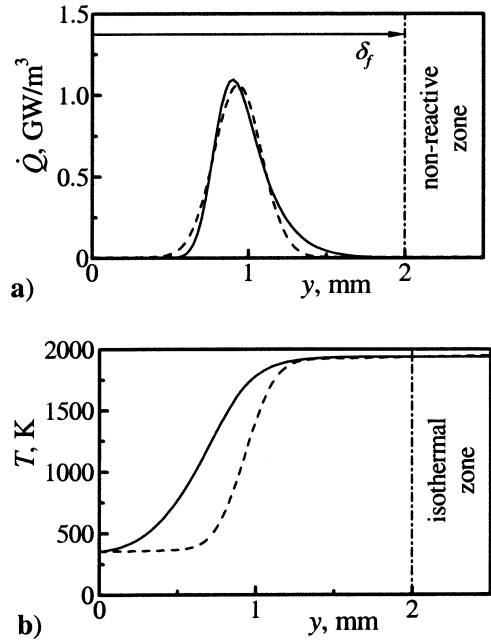


Fig. 1. Spatial distribution of a) the chemical rate of heat release $\dot{Q}(y)$, and b) the steady-state temperature $T(y)$ based on computational fluid dynamics (—) and analytical solutions (---). Note that for $y > \delta_f$ the reaction heat released is negligible.

spatial evolution of the temperature, attention is turned to the thermally enhanced gas velocity directly above the flame edge. Using mass conservation and the ideal gas law under isobaric conditions, one finds that

$$v_f = \frac{\rho_w}{\rho_f} v_w = \frac{T_f}{T_w} v_w \quad (13)$$

Consequently, given the injection temperature and velocity at the wall, the key for determining the thermally enhanced velocity lies in the accurate prediction of the flame temperature T_f .

3. Discussion

Figure 1a compares the analytical solution for $\dot{Q}(y)$, given by Eq. 8, and the numerical prediction of [6,7]. Also shown in Fig. 1b are the temperature distributions obtained analytically, from Eq. 9, and numerically, based on [6,7]. While the analytical solution matches the simulated temperature at the wall, it closely approximates T_f at the flame edge (i.e., at $y = \delta_f$). Outside the flame zone, the numerical solution yields a constant temperature of 1938 K while Eq. 9 predicts 1935 K. Coincidentally, the analytical value

is closer to the flame temperature of 1915 K procured from NASA's CET93 [14]; this code utilizes more detailed chemical reactions than those employed in [6,7]. Note that, because the analytically predicted T_f is close to the assumed value used in Eq. 12, there is no need to re-evaluate the average specific heat. In the absence of a priori knowledge of T_f the following algorithm may be used: 0) assume T_f ; based on the reaction type; 1) calculate \bar{C}_p from Eq. 12; 2) calculate T_f from Eq. 9; and 3) repeat steps 1 to 2 until convergence.

It should be noted that, outside the flame zone, the analytical solution predicts a slightly increasing temperature in the inward direction. This is contrary to the numerical simulation results in [6,7] which predict a constant temperature throughout the chamber core. Interestingly, the slight increase in temperature outside the flame zone is often exhibited in laminar premixed flame profiles for methane-air mixtures and other combustibles described in [2] (cf. p. 272). At the outset, it appears that the simple analytical model presented here can faithfully reproduce the fundamental thermal trends confirmed in previous studies [1–4]. Further refinements are necessary to reduce its limitations and broaden its applicability.

In like fashion, the validity of Eq. 13 can be verified for the specific problem of propane-air combustion. Whereas the velocity at the flame edge is calculated in [6,7] to be $v_f = 1.15 \text{ ms}^{-1}$, the approximate analysis based on Eq. 13 yields 1.14 ms^{-1} . The 1% error in the analytical prediction may be deemed reasonable, considering its relative simplicity in comparison to the finer flame zone detail captured by computational measurements.

References

- [1] Kuo, K.K., Principles of Combustion, Wiley-Interscience, 1986.
- [2] S.R. Turns, An Introduction to Combustion: Concepts and Applications, 2nd ed., McGraw Hill, New York, 1996.
- [3] Glassman, I., Combustion, 3rd ed., Academic Press, 1996.
- [4] Lewis, B. and von Elbe, G., Combustion, Flames and Explosions of Gases, 3rd ed., Academic Press, 1987.
- [5] E. Mallard, H.L. Le Châtelier, Ann. Mines 4 (1883) 379–568.
- [6] Chu, W.-W., Dynamic Responses of Combustion to Acoustic Waves in Porous Chambers with Transpiration, PhD Thesis, Department of Mechanical Engineering, Pennsylvania State University, College Park, 1999.
- [7] Chu, W.-W., Yang, V. and Majdalani, J., *Combust. Flame* 133 (2003) 359–370.
- [8] G.A. Flandro, *J. Prop. Power* 11 (1995) 607–625.
- [9] J. Majdalani, *J. Prop. Power* 17 (2001) 355–362.
- [10] J.S. T'ien, *Combust. Sci. Technol.* 5 (1972) 47–54.
- [11] R. Borghi, M. Destriau, *Combustion and Flames: Chemical and Physical Principles*, Editions Technip, Paris, 1998, p. 114–115.
- [12] Warnatz, J., Maas, U. and Dibble, R. W., *Combustion*, 3rd ed., Springer, 2001, p. 30–31.
- [13] J.D. Buckmaster, G.S.S. Ludford, *Lectures on Mathematical Combustion*, Society for Industrial and Applied Mathematics, Philadelphia, 1983, p. 40–41.
- [14] McBride, B.J. and Gordon, S., CET93 and CETPC: An Interim Updated Version of the NASA Lewis Computer Program for Calculating Complex Chemical Equilibria with Applications, TM-4557, NASA, Technical Report, 1994.